

I001

Modelling Anisotropy Pattern of Dry Rocks as a Function of Applied Stress

M. Madadi* (Curtin University), M. Pervukhina (CSIRO ESRE) & B. Gurevich (Curtin University / CSIRO ESRE)

SUMMARY

We propose an analytical model for seismic anisotropy caused by application of an anisotropic stress to an isotropic dry rock. We first consider an isotropic linearly elastic medium (porous or non-porous) permeated by a distribution of discontinuities with random (isotropic) orientation (such as randomly oriented compliant grain contacts or cracks). Geometry of individual discontinuities is not specified. Instead, their behaviour is defined by a ratio of the normal to tangential excess compliances. When this isotropic rock is subjected to a small compressive stress (isotropic or anisotropic), the specific surface area of cracks aligned parallel to a particular plane is reduced in proportion to the normal stress traction acting on that plane. This effect is modelled using the Sayers-Kachanov non-interactive approximation. The integral over the orientation distribution is evaluated using Taylor expansion of the stress dependency of the specific surface area of cracks. Comparison of the model predictions with the results of laboratory measurements shows a reasonable agreement for moderate magnitudes of uniaxial stress (up to 30 MPa). The results suggest that the relations between anisotropy parameters do not change with increasing stress.

Introduction

Stresses affect elastic properties of rocks due to presence of discontinuities such as cracks and compliant grain contacts. Non-hydrostatic stress can cause elastic anisotropy, since the effect of a stress field on a discontinuity depends on the orientation of the discontinuity with respect to the stress field. Knowledge of the pattern of stress-induced anisotropy (expressed, for example, by the ratio of anisotropy parameters) can be useful for distinguishing it from other causes of anisotropy, such as presence of larger-scale aligned fractures. Such patterns can also be used to estimate, say, P-wave anisotropy from S-wave anisotropy estimated from S-wave splitting.

A number of authors have modeled stress-induced anisotropy by assuming the rock to contain an isotropic random distribution of discontinuities, and considering variation of this distribution due to applied stress (Mavko *et al.*, 1995; Sayers, 1988, 2007). These approaches require numerical calculations to obtain an insight into anisotropy patterns. To obtain a simpler and more intuitive insight into these patterns, Gurevich *et al.* (2011) made some simplifying assumptions that lead to analytical expressions for the anisotropy parameters. Their main assumption was that the rock containing an isotropic distribution of discontinuities was subjected to a small uniaxial stress (or uniaxial strain) such that it results in a weak anisotropy of the discontinuity orientation distribution, and weak elastic anisotropy. Under this assumption, Gurevich *et al.* (2011) derived the following expressions for the ratios of anisotropy parameters

$$\frac{\varepsilon}{\delta} = 1 \quad (1)$$

and

$$\frac{\varepsilon}{\gamma} = 2 \frac{2\nu B + 6B - 2\nu + 1}{(1 - \nu)(3 + 4B)}, \quad (2)$$

where ν is Poisson's ratio of the unstressed rock, and B is the ratio of normal to tangential compliance of individual cracks. The result that ε/δ tends to 1 in the limit of small stress implies that the anisotropy is elliptical. This result is consistent with the general theory of nonlinear elasticity (Rasolofosaon, 1998).

The anisotropy pattern described by equations (1)-(2) is limited to small stresses. It is thus interesting and important to explore how these anisotropy patterns change for larger anisotropic stresses. To this end, in this paper we extend the analysis of Gurevich *et al.* (2011) to larger stresses.

Theoretical Model

Compliance tensor of a cracked solid

We first consider an isotropic elastic medium (porous or non-porous). We then assume that this medium at ambient stress is permeated by a distribution of cracks with random (isotropic) orientation. The exact geometry of individual cracks is not specified. Instead, the behaviour of cracks is defined by a ratio B of the normal B_N to tangential B_T excess crack compliances. All cracks are assumed identical; thus B is the same for all cracks. When this isotropic rock is subjected to a small compressive stress (isotropic or anisotropic), the number of cracks along a particular plane is reduced in proportion to the normal stress traction acting on that plane. In particular, if the stress is a uniaxial compression along the x axis, then the number of cracks normal to x axis will reduce most, while the number of cracks parallel to x axis will not reduce at all. We model this effect using the Sayers and Kachanov (1995) non-interactive approximation. According to Sayers and Kachanov (1995), the compliance tensor S_{ijkl} of a rock with a given distribution of linear-slip cracks (Schoenberg (1980)) can be written as

$$S_{ijkl} = S_{ijkl}^0 + \frac{1}{4} \left(\delta_{ik} \alpha_{jl} + \delta_{il} \alpha_{jk} + \delta_{jk} \alpha_{il} + \delta_{jl} \alpha_{ik} \right) + \beta_{ijkl}, \quad (3)$$

Here, S_{ijkl}^0 is the compliance tensor of the intact rock (no cracks), α_{ij} and β_{ijkl} are second and fourth-rank

tensors defined by

$$\alpha_{ij} = \frac{1}{V} \sum_r B_T^{(r)} n_i^{(r)} n_j^{(r)} A^{(r)} \quad \text{and} \quad \beta_{ijkl} = \frac{1}{V} \sum_r (B_N^{(r)} - B_T^{(r)}) n_i^{(r)} n_j^{(r)} n_k^{(r)} n_l^{(r)} A^{(r)}, \quad (4)$$

where $B_N^{(r)}$ and $B_T^{(r)}$ are the normal and shear compliances of the r -th crack in volume V , $n_i^{(r)}$ is the i -th component of the normal to the crack, and $A^{(r)}$ is the area of the crack. $B_N^{(r)}$ characterises the normal displacement jump across the crack produced by a unit normal traction, while $B_T^{(r)}$ characterises the shear displacement jump produced by a unit shear traction. The cracks are assumed to be rotationally symmetric, that is, $B_T^{(r)}$ is assumed to be independent of the direction of the shear traction within the plane of the crack. In equations (3)-(4), the cumulative effect of many cracks is assumed additive. In other words, interaction between cracks is neglected (the so-called non-interactive approximation, which is valid for a dilute concentration of cracks).

Effect of stress on crack distribution

To model closure of cracks due to application of anisotropic stress, we assume that $B_N^{(r)}$ and $B_T^{(r)}$ are the same for all cracks, while the total area $S = \sum_r A^{(r)}$ of cracks with a particular orientation (and specific area $s = S/V$ of cracks with that orientation) varies with the direction of the crack normal, and is an exponential function of the normal stress acting in that direction, as $s = s^0 \exp(\sigma_n/P_c)$, where s^0 is the specific area of all the cracks before application of anisotropic stress, $\sigma_n = \sigma_{ij} n_i n_j$ is normal stress traction acting on the crack surface, and P_c is a characteristic crack closing pressure (Schoenberg, 2002; Shapiro, 2003). Then summation in equations (4) can be written in integral form; for example, α_{ij} can be written as:

$$\alpha_{ij} = \frac{Z_{T0}}{4\pi} \int \int \exp\left(\frac{\sigma_n}{P_c}\right) n_i n_j d\Omega, \quad (5)$$

where $d\Omega$ is a body angle element and $Z_{T0} = s_0 B_T$. If $\sigma_n \ll P_c$ then the exponential in (5) can be linearised and the intergral can be evaluated analytically (Gurevich *et al.*, 2011). For larger stresses, α_{ij} can be calculated from the Taylor expansion of exponential functions. This gives the following closed form of the variation of the complinace tensor from isotropic part:

$$S = S^0 + Z_{T0} \begin{bmatrix} \mathbf{A} & \mathbf{0} \\ \mathbf{0} & \mathbf{B} \end{bmatrix} \quad (6)$$

where \mathbf{A} , and \mathbf{B} are matrices given by

$$\mathbf{A} = \begin{bmatrix} (2B\mathcal{G}(p) + (3B+2)\mathcal{F}(p)) & (B-1)\mathcal{F}(p) & (B-1)\mathcal{F}(p) \\ (B-1)\mathcal{F}(p) & \frac{(2\mathcal{G}(p) + (2+3B)\mathcal{F}(p))}{3} & \frac{(B-1)\mathcal{F}(p)}{3} \\ (B-1)\mathcal{F}(p) & \frac{(B-1)\mathcal{F}(p)}{3} & \frac{(2\mathcal{G}(p) + (2+3B)\mathcal{F}(p))}{3} \end{bmatrix}, \quad (7)$$

and

$$\mathbf{B} = \begin{bmatrix} \frac{2(2\mathcal{G}(p) + (3+2B)\mathcal{F}(p))}{3} & 0 & 0 \\ 0 & \frac{4(2\mathcal{G}(p) + (2+3B)\mathcal{F}(p))}{3} & 0 \\ 0 & 0 & \frac{4(2\mathcal{G}(p) + (2+3B)\mathcal{F}(p))}{3} \end{bmatrix}, \quad (8)$$

where p is the magnitude of the applied uniaxial stress and functions $\mathcal{F}(p)$ and $\mathcal{G}(p)$ are:

$$\mathcal{F}(p) = -\frac{1}{240} \left(16 - 90e^{-p} p^{-2} + 15\sqrt{\pi} \operatorname{erf}(\sqrt{p}) \left(3p^{-5/2} - 2p^{-3/2} \right) \right), \quad (9)$$

and,

$$\mathcal{G}(p) = -\frac{1}{32} \left((8p^{-1} + 30p^{-2}) e^{-p} - 3\sqrt{\pi} \operatorname{erf}(\sqrt{p}) \left(5p^{-5/2} - 2p^{-3/2} \right) \right). \quad (10)$$

Laboratory Example

To illustrate the analytical model derived above, we use the laboratory data of Nur and Simmons (1969) on a sample of Barre Granite. This data set was previously used to test the modeling approach of Mavko *et al.* (1995) and Gurevich *et al.* (2011), and is attractive because velocities were measured for a range of angles to the axis of symmetry, rather than for only 0, 45 and 90 degrees as is often the case.

To test our model against the laboratory data of Nur and Simmons (1969), we first need to determine the parameters of the model. Although a number of parameters were involved in deriving the anisotropy model, all of them can be grouped into five independent parameters: bulk and shear moduli of the unstressed rock K and μ , ratio of normal to tangential compliance B , the tangential compliance Z_{T0} , and crack closing pressure P_c .

To calculate these parameters, we fit the angle dependent phase velocities calculated from the exact analytical expressions for compliance tensor, equations (6)-(10), to experimental velocities by least square algorithm. The values of the parameters obtained are $K = 13.76\text{GPa}$, $\mu = 18.19\text{GPa}$, $\nu = 0.0412$, $B = 0.8989$, $P_c = 11.86\text{MPa}$, and $Z_{T0} = 0.0393\text{GPa}^{-1}$.

Figures 1(a-b) show corresponding velocities as functions of the angle to the symmetry axis for a number of pressure levels. The predictions capture the main trends of the experimental data but underestimate the magnitude of the P-wave anisotropy, probably due to opening of cracks parallel to the axis of applied stress, the phenomenon described by Sayers (1988).

To further explore the consistency of our model with the measured data, we estimate Thomsen's anisotropy parameters for Barre Granite from angle dependencies of P, SH and SV wave velocities measured by Nur and Simmons (1969). The sample is assumed to be transversely isotropic with a symmetry axis along the direction of uniaxial stress. These parameters as well as model predictions are shown in Figure 2 as functions of uniaxial stress.

Conclusions

We have presented a simple approach to modelling elastic anisotropy caused by application of a uniaxial stress to an isotropic rock. The main feature of the model is that it has only five parameters. Application of the model to a set of laboratory measurements of angle-dependent ultrasonic velocities on a granite sample provides a good fit. Furthermore for this specific sample, the model predicts almost the same anisotropy pattern as the model limited to small stresses. In particular, the anisotropy remains almost elliptical for large stresses. These predictions however may change when the compliance ratio of discontinuities $B = B_N/B_T$ deviates from 1 more significantly.

References

Gurevich, B., Pervukhina, M., and Makarynska, D., [2011], An analytic model for the stress-induced anisotropy of dry rocks, *Geophysics*, **76**, WA125, DOI:10.1190/1.3567950

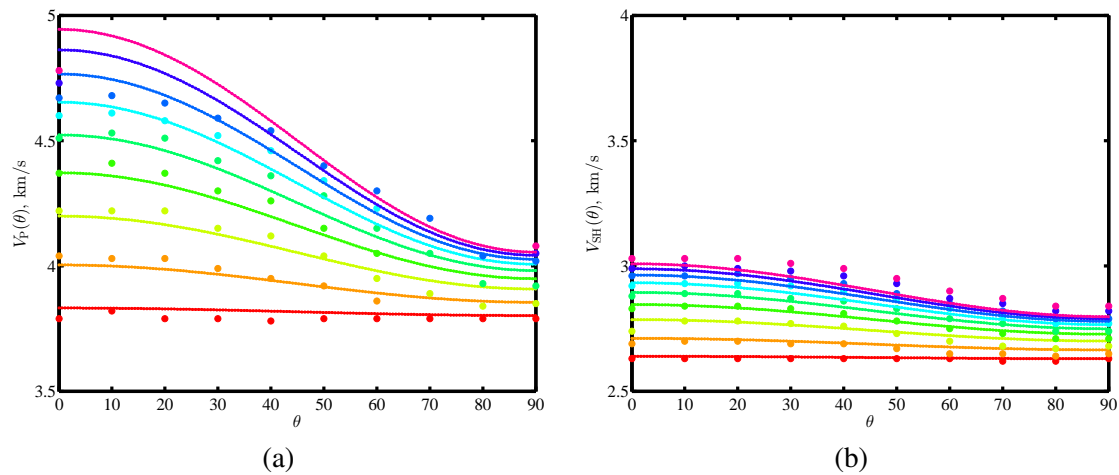


Figure 1 Comparison of angle dependencies of measured velocities of P, and SH waves and model predictions for a sample of Barre Granite subjected to different levels of uniaxial stress.

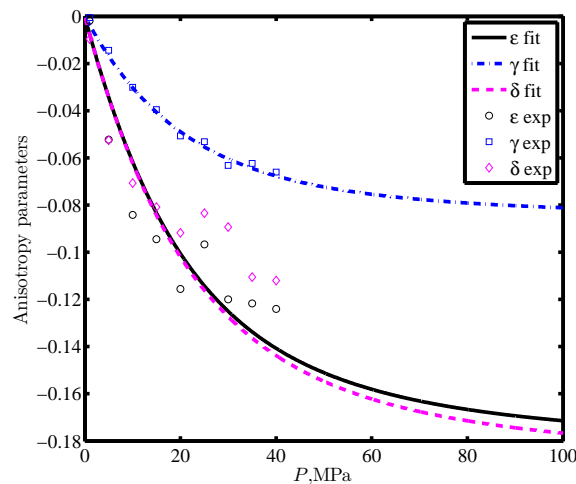


Figure 2 Thomsen's anisotropy parameters ϵ (black line), γ (blue line) and δ (pink line) versus uniaxial stress for Barre Granite as estimated from angle dependencies of P, SH and SV. Symbols are corresponding anisotropy parameters extracted directly from ultrasonic velocities for each stress level.

- Mavko, G., Mukerji, T., and Godfrey, N., [1995], Predicting stress-induced velocity anisotropy in rocks, *Geophysics*, **60**, 1081-1087.
- Nur, A., and Simmons, G., [1969], Stress-induced velocity anisotropy in rock: An experimental study: *Journal of Geophysical Research*, **74**, 6667-6674.
- Rasolofosaon, P., [1998], Stress-induced seismic anisotropy revisited: *Oil & Gas Science and Technology - Rev. IFP*, **53**, No. 5.
- Sayers, C. M., [1988], Stress-induced ultrasonic wave velocity anisotropy in fractured rock: *Ultrasonics*, **26**, 311-317.
- Sayers, C. M., [2007], Effects of borehole stress concentration on elastic wave velocities in sandstones: *International Journal of Rock Mechanics & Mining Sciences*, **44**, 1045-1052.
- Sayers, C. M., and Kachanov, M., [1995], Microcrack-induced elastic wave anisotropy of brittle rocks: *Journal of Geophysical Research*, **100**, 4149-4156.
- Schoenberg, M. A., [1980], Elastic wave behavior across linear slip interfaces: *Journal of the Acoustical Society of America*, **68**, No. 5, 1516-1521.
- Schoenberg, M. A., [2002], Time-dependent anisotropy induced by pore pressure variation in fractured rock: *Journal of Seismic Exploration*, **11**, 83-105.
- Shapiro, S. A., [2003], Elastic piezosensitivity of porous and fractured rocks: *Geophysics*, **68**, 482-486.